An Effective Implementation of Reliability Methods for Bayesian Model Updating of Structural Dynamic Models with Multiple Uncertain Parameters

D. J. Jerez[1], H. A. Jensen[2], and M. Beer[1,3,4]

[1]*Institute for Risk and Reliability, Leibniz Universität Hannover, 30167 Hannover, Germany.*

[2]*Departamento de Obras Civiles, Universidad Técnica Federico Santa María, 2390302 Valparaiso, Chile*

[3]*International Joint Research Center for Engineering Reliability and Stochastic Mechanics, Tongji University, 200092 Shanghai, China.*

[4]*Institute for Risk and Uncertainty and School of Engineering, University of Liverpool, Liverpool L69 7ZF, United Kingdom.*

Abstract

The use of reliability methods in the framework of Bayesian model updating of structural dynamic models using measured responses is explored for high-dimensional model parameter spaces. This formulation relies on a recently established analogy between Bayesian updating problems and reliability problems. Under this framework, samples following the posterior distribution of the Bayesian model updating problem can be obtained as failure samples in an especially devised reliability problem. An approach that requires only minimal modifications to the standard subset simulation algorithm is proposed and implemented. The scheme uses an adaptive strategy to select the threshold value that determines the last subset level. Due to the basis of the formulation, the approach does not make use of any problem-specific information and, therefore, any type of structural model can be considered. Furthermore, no prior knowledge on the maximum likelihood function value is required by the proposed scheme. The approach is combined with an efficient parametric model reduction technique for an effective numerical implementation. The performance of the proposed implementation is assessed numerically for a linear building model and a nonlinear three-dimensional bridge structural model. The results indicate that the proposed implementation represents an effective numerical technique to address high-dimensional Bayesian model updating problems involving complex structural dynamic models.

Keywords: Bayesian analysis, Identification, Markov chain Monte Carlo, Model updating,

Reliability analysis, Structural dynamics, Subset simulation.

1. Introduction

Model updating of structural dynamic models using measured responses has a significant number of applications in robust structural response prediction, reliability and sensitivity analyses, structural control, structural health monitoring, etc. Moreover, the appropriate evaluation of the state of structures over their lifetime based on measurements is an important and challenging task in structural engineering applications [1, 2, 3, 4, 5, 6]. For a proper assessment of updated models all uncertainties involved in the problem need to be considered. In this regard, a fully probabilistic Bayesian model updating approach provides a robust and rigorous framework for model updating due to its ability to characterize uncertainties associated with the underlying structural dynamic system and update the corresponding distribution based on available data about the structural behavior [7, 8, 9].

For problems of practical interest, the Bayesian approach requires the evaluation of multi-dimensional integrals which cannot be done analytically. One way to address this difficulty is to use a Gaussian approximation to the posterior probability density function by means of the Laplace method of asymptotic approximation [10]. This type of methods requires to identify the point in the uncertain parameter space which yields the maximum likelihood value and to evaluate the corresponding Hessian matrix of the likelihood function [11, 12]. Such approach has been used in the past and it is usually valid when there is a large amount of data and the model is globally identifiable. However, the application of this approximation faces some problems in practical cases when the amount of data is not sufficient or when the problem is unidentifiable based on the available information [13]. A more general approach is to use stochastic simulation methods in which samples consistent with the posterior probability density function are generated. Some potential difficulties related to this approach are associated with the evaluation of the so-called evidence, which requires a high-dimensional integration over the uncertain parameter space. Moreover, the high probability content of the posterior probability density function frequently occupies a very small volume compared with that of the prior probability density function. Therefore, the required samples cannot be generated efficiently by sampling from the prior probability density function using direct Monte Carlo simulation. To tackle the previous difficulties, Markov chain Monte Carlo (MCMC) methods have been proposed to solve Bayesian model updating problems more efficiently [14, 15]. In this framework, the most well-known MCMC method is the Metropolis-Hastings (MH) algorithm [16, 17]. The method creates samples from a Markov chain whose stationary state is a specified target probability density function, which corresponds to the posterior distribution. Though this algorithm is quite general, its direct implementation is usually inefficient since the high probability content tends to concentrate in a small volume of the parameter space, as indicated before. To improve the effectiveness of the method, an approach based on the MH algorithm and simulated annealing concepts was proposed in [18]. The main idea is to simulate from a sequence of target probability density functions which converges to the posterior distribution. For each level, a kernel sampling density based on results from the previous level is used as global proposal distribution to simulate samples efficiently. However, this strategy requires a prohibitively large number of samples for higher dimensions. An effective method that adopts the idea as in [18] of using a sequence of intermediate distributions, called the transitional Markov chain Monte Carlo (TMCMC) method, was proposed in [19]. Instead of using kernel sampling densities, the method relies on a combination of reweighting, resampling and random walk strategies to obtain samples during each level. The approach is more efficient and, in addition, it allows the estimation of the evidence as a byproduct of the simulation process. However, the TMCMC method has potential problems in higher dimensions since, in such cases, the convergence to the target probability density function can be very slow and the corresponding statistical estimates can be biased [20].

To handle high-dimensional Bayesian model updating problems of structural dynamic models using measured responses, sampling schemes based on fictitious dynamic systems have been implemented [20, 21]. These methods rely on the introduction of an auxiliary dynamic system whose potential energy function is defined in terms of the posterior distribution of the model parameters, which allows to exploit the structure of the identification problem. The implementation of this class of algorithms involves the calibration of a number of parameters associated with the characterization and numerical solution of the fictitious dynamic system [20, 21, 22] and, in addition, they unavoidably require taking derivatives of the likelihood function with respect to the identification parameters. Additional methods that have been suggested for this type of identification problems include subspace identification techniques [23] and Kalman-filtering-based approaches [24, 25]. Finally, another approach that in principle can handle problems involving a large number of uncertain parameters is based on structural reliability methods [26]. In this case, the idea is to build an analogy between Bayesian updating problems and reliability problems. In this context, samples following the posterior distribution in the Bayesian updating problem can be obtained as failure samples in an equivalent reliability problem. This approach, referred to as BUS (Bayesian updating with structural reliability methods), has been considered in [26] where the posterior samples are obtained as the conditional samples in subset simulation [27, 28] at the highest simulation level. One of the difficulties of this approach is the proper choice of the so-called likelihood multiplier connected with the rejection principle [29] involved in its formulation. In this regard, several approaches have been suggested to address this issue. They include an approach based on a postprocessing step to correct the distribution of failure samples [30], an inner-outer subset simulation approach [31], and an approach that adaptively modifies the limit-state function during subset simulation [32].

The previous procedures, which are well established, have been applied to a variety of problems, including analytical problems with high-dimensional parameter spaces, nonlinear static systems, reliability-based monitoring sensitivity analysis for reinforced slopes, and structural dynamic models with relatively few parameters [33, 34, 35]. However, studies on the effectiveness of BUS approaches to handle structural dynamic systems have been limited to academic-type of problems. Furthermore, high-dimensional Bayesian model updating of complex structural dynamic systems remains a significantly important challenge in the assessment and life-cycle management of existing structures. Thus, there is a necessity for developing not only sound theoretical algorithms to address this class of problems, but also the appropriate techniques for implementing such procedures in engineering practice. Given that dimension sustainability is efficiently handled by advanced simulation techniques, it is the objective of this work to propose an effective implementation of structural reliability methods in the context of Bayesian model updating of complex structural dynamic models involving measured response data and multiple uncertain parameters.

As previously pointed out, this type of problems has not been addressed by previous contributions in the framework of BUS. Subset simulation, a well established sampling technique, is implemented in this work by combining some of the ideas introduced in [31, 32]. The resulting algorithm uses an adaptive strategy to select the threshold value that determines the last subset level, where samples beyond such threshold follow the posterior distribution of the original Bayesian updating problem. In this setting, only minimal modifications to the standard subset simulation algorithm are required. At the same time, the approach effectively avoids the necessity of prior knowledge on the maximum value of the likelihood function, the need to redefine the limit-state function during each level of subset simulation, and the iterative solution of an inner reliability problem during the sampling process. Overall, the proposed method represents an effective numerical technique for the treatment of Bayesian identification problems involving complex, realistic and practical structural models and multiple uncertain parameters.

The structure of the paper is as follows. In Section 2, the use of structural reliability methods in the framework of Bayesian model updating is reviewed. The solution of the corresponding reliability problem is discussed in Section 3. Implementation aspects of the proposed scheme are addressed in Section 4. In Section 5, example problems involving structural dynamic models with multiple uncertain parameters are presented to demonstrate the applicability of the proposed implementation. Conclusions are presented in Section 6.

2. Background

2.1. Bayesian Model Updating Problem

Let $\boldsymbol{\theta} \in \boldsymbol{\Theta} \subset R^{n_{\boldsymbol{\theta}}}$ be the set of parameters of a model class M. The objective of model updating is to compute the posterior probability density function of the model parameters $p(\boldsymbol{\theta}|M, D)$ using available data D [7, 10]. According to Bayes' Theorem, the posterior probability density function of $\boldsymbol{\theta}$ is given by

$$p(\boldsymbol{\theta}|M, D) = \frac{L(D|M, \boldsymbol{\theta})\, p(\boldsymbol{\theta}|M)}{P(D|M)} \tag{1}$$

where $L(D|M, \boldsymbol{\theta})$ is the likelihood function, $p(\boldsymbol{\theta}|M)$ is the prior probability density function of $\boldsymbol{\theta}$, and $P(D|M)$ is the evidence of model class M. The likelihood function expresses the plausibility of observing the data D given a certain value of $\boldsymbol{\theta}$, while the prior probability density function represents the prior or initial belief about the distribution of $\boldsymbol{\theta}$. Moreover, the evidence of the model class is written as

$$P(D|M) = \int_{\Theta} L(D|M, \boldsymbol{\theta})\, p(\boldsymbol{\theta}|M) d\boldsymbol{\theta} \tag{2}$$

which can be used for Bayesian model class selection [36] and model averaging [37]. To simplify the notation, Eq. (1) is rewritten as

$$p(\boldsymbol{\theta}|D) = P(D)^{-1} L(\boldsymbol{\theta})\, p(\boldsymbol{\theta}) \tag{3}$$

where $p(\boldsymbol{\theta}|D)$ denotes the posterior probability density function, $L(\boldsymbol{\theta})$ denotes the likelihood function, $p(\boldsymbol{\theta})$ denotes the prior probability density function, and $P(D)$ denotes the evidence. It is noted that the posterior distribution cannot be derived analytically for general cases and, therefore, posterior samples are usually generated by means of stochastic simulation techniques. Finally, in the context of the present work it is assumed that D contains input dynamic data and output responses from measurements on the structural system.

2.2. Mechanical Modeling

The class of structural systems under consideration is characterized by a multi-degree of freedom model satisfying the equation of motion

$$\mathbf{M}\ddot{\mathbf{x}}(t) \;+\; \mathbf{C}\dot{\mathbf{x}}(t) \;+\; \mathbf{K}\mathbf{x}(t) + \mathbf{f}_{NL}(\mathbf{x}(t), \dot{\mathbf{x}}(t), \boldsymbol{\tau}(t)) \;=\; \mathbf{f}(t) \tag{4}$$

where $\mathbf{x}(t)$ denotes the displacement vector of dimension n_x, $\mathbf{f}_{NL}(\mathbf{x}(t), \dot{\mathbf{x}}(t), \boldsymbol{\tau}(t))$ the vector of nonlinear restoring forces, $\boldsymbol{\tau}(t)$ the set of variables which describe the state of the nonlinear components, and $\mathbf{f}(t)$ the external force vector. The matrices $\mathbf{M}$, $\mathbf{C}$, and $\mathbf{K}$ describe the mass, damping, and stiffness, respectively. The evolution of the set of variables $\boldsymbol{\tau}(t)$ is described by an appropriate nonlinear model which depends on the nature of the nonlinearity. Note that the previous equation of motion constitutes a dynamic system with localized nonlinearities, which can also be extended to other cases such as the consideration of nonlinear models for the structure.

2.3. Likelihood Function

Let $r_n(t_j, \boldsymbol{\theta})$ denote the response of interest at time t_j at the n^{th} observed degree of freedom predicted by the structural model corresponding to the parameters $\boldsymbol{\theta}$, and $r_n^*(t_j)$ denotes the corresponding measured output. The prediction and measurement errors $e_n(t_j, \boldsymbol{\theta}) = r_n^*(t_j) - r_n(t_j, \boldsymbol{\theta})$ for $n = 1, \ldots, n_o$, and $j = 1, \ldots, n_t$, where n_o denotes the number of observed degrees of freedom and n_t denotes the length of the discrete time history data, are modeled as independent and identically distributed Gaussian variables with zero mean and variance σ^2 [36]. This assumption implies stochastic independence of the errors for different channels of measurements and for different time instants. In this regard, it is noted that alternative prediction error model classes can be used as well [38]. Using the above probability model for the prediction and measurement errors, the likelihood function $L(\boldsymbol{\theta})$ can be expressed as [10, 13, 36]

$$L(\boldsymbol{\theta}) = \frac{1}{(2\pi\sigma^2)^{n_o n_t/2}} \exp\left[-\frac{1}{2\sigma^2} J(\boldsymbol{\theta})\right] \quad (5)$$

where

$$J(\boldsymbol{\theta}) = \sum_{n=1}^{n_o} \sum_{j=1}^{n_t} \left(r_n^*(t_j) - r_n(t_j, \boldsymbol{\theta})\right)^2 \quad (6)$$

is a measure-of-fit function between the measured response and the model prediction at the measured degrees of freedom. In the context of the previous equation it is noted that different types of response quantities can be used to define the measure-of-fit function.

2.4. Equivalent Reliability Problem

As previously pointed out, simulation-based Bayesian model updating techniques such as Markov chain Monte Carlo methods provide a powerful computational tool for generating posterior samples. In particular, the TMCMC method has proved to be efficient in generating samples asymptotically distributed as the posterior probability density function for low/intermediate-dimensional Bayesian model updating problems [19, 39, 40]. However, MCMC methods may encounter difficulties in connection with their efficiency and stability as the dimension of the problem increases. To handle these potential difficulties, a framework that converts the generation of posterior samples into the task of obtaining failure samples associated with an equivalent reliability problem has been suggested and explored in [26, 30, 31, 32].

The basic idea of Bayesian updating with structural reliability methods, as suggested in [26], is to transform the identification problem into a reliability problem. To this end, define a failure event F in the form

$$F = \{u < cL(\boldsymbol{\theta})\} = \{cL(\boldsymbol{\theta}) - u > 0\} \quad (7)$$

where u is an auxiliary random variable uniformly distributed on $[0, 1]$ with probability density function $I_{[0,1]}(u)$, and $\boldsymbol{\theta}$ is the set of uncertain model parameters with probability density function $p(\boldsymbol{\theta})$. Note that the distribution of the model parameters associated with the failure event stated in Eq. (7) is actually the prior distribution of the Bayesian model updating problem defined in Eq. (1), i.e., $p(\boldsymbol{\theta})$. The constant $c > 0$ corresponds to the so-called likelihood multiplier, which must satisfy the inequality [29]

$$cL(\boldsymbol{\theta}) \leq 1 \;\text{ or }\; c^{-1} \geq L(\boldsymbol{\theta}), \;\text{ for all } \boldsymbol{\theta} \in \boldsymbol{\Theta} \tag{8}$$

If failure samples distributed as $p(\boldsymbol{\theta})I_{[0,1]}(u)$, conditional on the failure event F can be generated by means of any simulation technique, then such samples follow the posterior distribution $p(\boldsymbol{\theta}|D)$. In addition, the evidence of the model class, $P(D)$, can be also computed in this framework as

$$P(D) = c^{-1}P_F \tag{9}$$

where P_F is the probability of failure event F and c^{-1} satisfies Eq. (8). More details on the derivation of the previous results can be found, e.g., in [26, 31].

2.5. Likelihood Multiplier

From Eq. (8) it is clear that the smallest admissible value of c^{-1}, i.e., c^{-1}_{adm}, is given by

$$c^{-1}_{adm} = \max_{\boldsymbol{\theta} \in \boldsymbol{\Theta}} L(\boldsymbol{\theta}) \tag{10}$$

Generally, this value is not known in advance and it is numerically challenging to choose a likelihood multiplier that guarantees the inequality $cL(\boldsymbol{\theta}) \leq 1$ for all $\boldsymbol{\theta}$. On the one hand, using a value larger than c^{-1}_{adm} will give the correct posterior distribution at the expense of decreasing the efficiency of the sample generation process. On the other hand, using a value smaller than c^{-1}_{adm} will lead to bias in the distribution of the samples. Thus, an appropriate choice of this parameter is crucial as it affects the definition of the failure event F in Eq. (7). In this regard, several approaches have been suggested for addressing the proper selection of the multiplier. They include an approach based on a postprocessing step to correct the sampling results [30], an inner-outer subset simulation approach [31], and an approach that adaptively modifies the limit-state function during subset simulation [32]. An additional discussion about these approaches is provided in Section 3.6. Finally, it is noted that in some cases it is possible to study the structure of $L(\boldsymbol{\theta})$ and derive a value of the likelihood multiplier that guarantees $cL(\boldsymbol{\theta}) \leq 1$ [26], although it is not necessarily the optimal value. Clearly, the use of these approximations can be computationally advantageous in such particular situations. Nonetheless, the optimal value of the likelihood multiplier, which is associated with the maximum likelihood value, is difficult to determine for general cases of practical interest, as already pointed out. In this regard, an alternative approach that effectively avoids the a priori definition of this quantity is described in the next section.

3. Solution of Equivalent Reliability Problem

As indicated in the previous section, any structural reliability method can be used to solve the equivalent reliability problem. In particular, subset simulation is of special interest since it is efficient and effective for handling problems involving small failure probabilities. In addition, its performance does not depend on the number of uncertain parameters involved in the problem, it is not restricted to specific types of structural systems, and its robustness and efficiency have been demonstrated in a wide variety of applications. This advanced simulation technique generates samples conditional on a sequence of intermediate failure events. Such samples are generated by MCMC and they gradually populate the target failure region, while the intermediate failure events are adaptively defined during the sampling process. In this contribution, subset simulation is implemented to generate failure samples associated with the equivalent reliability problem. The proposed technique effectively avoids a priori definitions of the likelihood multiplier, the need to redefine the driving variable during each simulation level, and the solution of inner reliability problems during the sampling process. Finally, the reader is referred to [27, 28] for a detailed description, from the theoretical and implementation viewpoints, of subset simulation for reliability analysis.

3.1. Preliminary Observations

As previously pointed out, subset simulation is adopted to obtain samples following the posterior distribution $p(\boldsymbol{\theta}|D)$. To this end, and following some of the ideas presented in [31, 32], the failure event defined in Eq. (7) is first rewritten as

$$F = \{v(\boldsymbol{\theta}, u) > v^{th}\} \tag{11}$$

with

$$v(\boldsymbol{\theta}, u) = \ln\left(\frac{L(\boldsymbol{\theta})}{u}\right) \quad , \quad v^{th} = \ln(c^{-1}) \tag{12}$$

where $\ln(\cdot)$ denotes natural logarithm. Note that in the previous formulation, the driving variable v does not depend on the value of the multiplier c. Moreover, the multiplier only affects the threshold level v^{th} and, therefore, subset simulation can be performed without the necessity of specifying the value of the multiplier beforehand. In principle, as long as the multiplier satisfies the inequality in Eq. (8), the marginal distribution of $\boldsymbol{\theta}$ conditional on the failure event $F = \{v > v^{th}\}$ is equal to the posterior distribution $p(\boldsymbol{\theta}|D)$ [26, 31, 32]. Thus, the minimum value of v^{th} beyond which the samples theoretically follow the posterior probability density function is

$$v^{th}_{min} = \ln\left(\max_{\boldsymbol{\theta}\in\boldsymbol{\Theta}} L(\boldsymbol{\theta})\right) \tag{13}$$

This value, which is generally unknown, does not affect the subset simulation procedure. In fact, subset simulation can be performed until the intermediate threshold of the highest level has passed v^{th}_{min}. This is possible since the intermediate failure events in subset simulation are defined in terms of the driving variable values obtained during the sampling process, that is, their definition does not require information on the target threshold level v^{th}. An approach that adaptively estimates v^{th}_{min} based on the samples obtained during the different levels of subset simulation is described in what follows.

3.2. Synopsis of Proposed Scheme

Following the ideas of subset simulation, the first step (level 0) consists in drawing N samples $\{\boldsymbol{\theta}^0_i, u^0_i\}, i = 1, \ldots, N$ from the joint distribution $p(\boldsymbol{\theta})I_{[0,1]}(u)$. The likelihood function $L(\cdot)$ is evaluated at each sample and the initial threshold level of the reliability problem in Eq. (11) is selected as the logarithm of the maximum likelihood value, i.e., $v^{th} = \ln(\max_{i=1,\ldots,N} L(\boldsymbol{\theta}^0_i))$. Thereafter, each step is performed in accordance with the standard formulation of subset simulation with only a minor modification. At the end of each simulation level, say level k, the threshold level is updated based on the samples $\{\boldsymbol{\theta}^k_i, u^k_i\}, i = 1, \ldots, N$, obtained during such a level as $v^{th} \leftarrow \max\{v^{th}, \ln(\max_{i=1,\ldots,N} L(\boldsymbol{\theta}^k_i))\}$. Based on this updating scheme, it is clear that the threshold v^{th} can only increase after each iteration, providing better estimates of the optimum threshold level as the simulation continues. The iteration over the subset levels is performed until the standard stopping criterion of subset simulation is verified, that is, until the threshold associated with the current intermediate failure event surpasses the current threshold value. It is noted that a similar strategy is adopted in [32], but at the limit-state function level. In such approach, all limit-state function values are updated at the end of each subset level.

In the previous framework it is noted that the final value of $c^{-1} = \exp(v^{th})$, which is a stochastic quantity, corresponds to the largest likelihood value observed during the entire simulation. For large N, the value of c^{-1} asymptotically approaches to c_{adm}^{-1}, but for finite N, this parameter is very likely smaller than c_{adm}^{-1}. However, this fact does not impede the proposed scheme to produce samples that follow the posterior distribution from a practical viewpoint. In this regard, the number of samples employed in each level of subset simulation must be selected large enough to allow an effective exploration of the entire failure domain. Note that these samples will not necessarily identify the uncertain parameter values that maximize the likelihood function. Therefore, it is likely that the final value of c^{-1}, which corresponds to the maximum likelihood value observed during the entire sampling process, is such that $c^{-1} \leq c_{adm}^{-1}$, as previously pointed out. However, the important region of the likelihood function can be effectively explored by the proposed approach, as illustrated in the numerical examples presented in this contribution (see Section 5).

3.3. Underlying Normal Space

Regarding the numerical implementation of the proposed scheme, the reliability problem is first set in terms of an underlying normal space $\mathbf{Z} \subset R^{n_\theta+1}$ of independent standard normal variables following the standard formulation of subset simulation [27]. The mapping between the spaces $\mathbf{Z}$ and $\mathbf{\Theta} \times [0,1]$ can be obtained by means of several techniques [41, 42]. In fact, without loss of generality, the transformation between the first n_θ components of $\mathbf{z}$, denoted by $(\mathbf{z})_{1:n_\theta}$, and $\boldsymbol{\theta}$ can be written in terms of a transformation as $\boldsymbol{\theta} = \boldsymbol{\theta}((\mathbf{z})_{1:n_\theta})$. On the other hand, the uniformly distributed random variable u can be written in terms of the last component of $\mathbf{z}$, i.e., $(\mathbf{z})_{n_\theta+1}$, as $u = \Phi((\mathbf{z})_{n_\theta+1})$, where $\Phi(\cdot)$ is the cumulative distribution function of the standard normal distribution. Note that, however, an implementation of the reliability problem directly in the original space $\mathbf{\Theta} \times [0,1]$ is also possible.

3.4. Basic Procedure

In the following, a procedure that illustrates the basic implementation of subset simulation, in the context of the present formulation, is provided.

1. Define the conditional probability of the intermediate failure events p_0 and the number of samples N. These parameters are chosen such that $p_0 N$ is an integer number.
2. Generate N samples $\{(\mathbf{z}_{0,i}), i = 1, \ldots, N\}$ by direct Monte Carlo according to the standard multivariate normal distribution (the subscript 0 denotes that the samples correspond to the unconditional level, i.e., level 0).
3. Set $k = 1$ and $v^{th} = \max_{i=1,\ldots,N} \ln(L(\boldsymbol{\theta}_{0,i}))$, where $\boldsymbol{\theta}_{0,i} = \boldsymbol{\theta}((\mathbf{z}_{0,i})_{1:n_\theta})$.

4. Evaluate the driving variable v to obtain $\{v(\mathbf{z}_{k-1,i}), i = 1, \ldots, N\}$. Arrange these values in ascending order, where $v(\mathbf{z}_{k-1,i}) = \ln(L(\boldsymbol{\theta}_{k-1,i})/u_{k-1,i})$, $\boldsymbol{\theta}_{k-1,i} = \boldsymbol{\theta}((\mathbf{z}_{k-1,i})_{1:n_\theta})$, and $u_{k-1,i} = \Phi((\mathbf{z}_{k-1,i})_{n_\theta+1})$.
5. Identify the $[(1-p_0)N]$th largest value of the set $\{v(\mathbf{z}_{k-1,i}), i = 1, \ldots, N\}$. In case this value is equal or larger than v^{th}, set $m = k$, $v_m = v^{th}$ and go to step 9. Otherwise, set the intermediate threshold value v_k equal to the aforementioned $[(1-p_0)N]$th largest value of the set $\{v(\mathbf{z}_{k-1,i}), i = 1, \ldots, N\}$.
6. The kth intermediate failure domain is defined as $F_k = \{\mathbf{z} \in \mathbf{Z} | v(\mathbf{z}) > v_k\}$. The estimate for $P(F_k)$ (if $k = 1$) or $P(F_k/F_{k-1})$ (if $k > 1$) is equal to p_0 by construction.
7. By construction there are $p_0 N$ samples among $\{(\mathbf{z}_{k-1,i}), i = 1, \ldots, N\}$ whose driving variable values are larger than v_k. Starting from each of these conditional samples, the modified Metropolis-Hastings algorithm [27] is used to generate additional $(1-p_0)N$ conditional samples that lie in F_k making a total of N conditional samples $\{(\mathbf{z}_{k,i}), i = 1, \ldots, N\}$ at level k.
8. Set $v^{\text{aux}} = \max_{i=1,\ldots,N} \ln(L(\boldsymbol{\theta}_{k,i}))$, where $\boldsymbol{\theta}_{k,i} = \boldsymbol{\theta}((\mathbf{z}_{k,i})_{1:n_\theta})$. Update the threshold level as $v^{th} \leftarrow \max\{v^{th}, v^{\text{aux}}\}$. Return to step 4 with $k \leftarrow k + 1$.
9. The failure probability is estimated as

$$P_F \approx p_0^{m-1} \frac{1}{N} \sum_{i=1}^{N} I_{F_m}(\mathbf{z}_{m-1,i}) \tag{14}$$

   where $\{\mathbf{z}_{m-1,i}, i = 1, \ldots, N\}$ is the set of samples generated at the last stage of subset simulation (conditional level $m-1$), and $I_{F_m}(\mathbf{z}_{m-1,i})$ is the indicator function of F_m, with $I_{F_m}(\mathbf{z}_{m-1,i}) = 1$ if $\mathbf{z}_{m-1,i} \in F_m$ and $I_{F_m}(\mathbf{z}_{m-1,i}) = 0$ otherwise. The samples that lie in the target failure domain F_m follow the posterior distribution $p(\boldsymbol{\theta}|D)$.
10. The evidence is estimated as

$$P(D) \approx \exp(v^m) P_F \tag{15}$$

As indicated in step 7 of the above procedure, the modified Metropolis-Hastings algorithm [27] is implemented to generate conditional samples during each simulation level. In this regard, each component of the candidate sample is generated independently. A uniform distribution centered at the lead value is selected as the proposal distribution for each component. This choice, which is commonly adopted in the implementation of subset simulation for reliability assessment of structural dynamic systems, has proven effective to handle the numerical examples presented in this contribution. Based on the above procedure, it is clear that the proposed approach requires only minimal modifications to the standard formulation of subset simulation.

3.5. Potential Enhancements

Several additional enhancements can be implemented to improve the performance and computational efficiency of the proposed method. For example, the acceptance rate of the sampling process, in the framework of the modified Metropolis-Hastings algorithm, can be controlled by using adaptive proposal distributions [43]. Similarly, to decrease the dependency of the generated samples and, consequently, increase the overall performance of the scheme, resampling strategies for the auxiliary variable associated with the rejection sampling scheme can be considered [32]. Actually, the previous techniques have been implemented in the present formulation. Additionally, alternative definitions of the proposal distribution, in the context of the modified Metropolis-Hastings algorithm, can improve the performance of the sampling procedure for certain applications. Finally, variants of the basic formulation of subset simulation have also been proposed to improve its efficiency, e.g., [28, 44]. Certainly, such variants can also be considered in the framework of the present contribution.

3.6. Remarks on Proposed and Alternative BUS Implementations

Several approaches in the framework of BUS have been proposed. A direct implementation [26] and a postprocessing step to correct the final results [30] have been previously reported. Both methods require an initial choice of the likelihood multiplier, c, which can significantly affect their performance [30]. Alternatively, the approach presented in [31] iteratively updates the value of c in terms of the intermediate thresholds of subset simulation. The sampling process continues until the probability of the likelihood function exceeding the current value of c^{-1} is smaller than a user-defined tolerance. In practice, then, this approach indirectly defines the likelihood multiplier in terms of a certain quantile of the likelihood function. Besides, its formulation requires to solve an inner reliability problem in each stage of subset simulation. Finally, the approach presented in [32] iteratively updates the driving variable function, in the context of subset simulation, using the maximum observed likelihood value. The process continues until sufficient failure samples are obtained. Hence, the final value of c is defined using the effective support of the likelihood function instead of specifying it beforehand.

To avoid an a priori characterization of the likelihood multiplier, this work follows the strategy presented in [32]. That is, the final value of c^{-1} is equal to the maximum likelihood value observed throughout all subset simulation stages. However, to circumvent the iterative definition of the driving variable, the failure event is explicitly defined as in [31]. As previously pointed out, only minimal modifications to the standard subset simulation algorithm are needed and the iterative solution of inner reliability problems is avoided. Overall, the resulting method represents an alternative BUS approach which provides an effective treatment of the likelihood multiplier while maintaining simplicity in its formulation and implementation. This feature is particularly attractive from a practical viewpoint, especially in the context of Bayesian model updating problems involving structural dynamic systems with multiple uncertain parameters.

4. Implementation Aspects

4.1. Initial Remarks

The solution of the equivalent reliability problem involves a large number of model evaluations associated with the repeated evaluation of the likelihood function. In fact, this process is computationally very demanding due to the large number of dynamic analyses (in the order of thousands) required for populating the failure region. This is especially important when the computational time for performing a single dynamic analysis is significant. To cope with this difficulty, a number of strategies based on meta-modeling techniques have been considered [45, 46]. In the context of Bayesian updating using structural reliability methods, strategies based on surrogate models [47, 48] have been proposed at the limit state function level. It is noted that the previous approaches have been demonstrated in applications involving structural dynamic systems with relatively few model parameters. In general, the effective integration of surrogate models for higher-dimensional parameter spaces remains one of the main challenges in Bayesian model updating applications.

4.2. Parametric Model Reduction Technique

Considering that the focus of this work is on Bayesian model updating of structural dynamic models with multiple uncertain parameters and measured responses, an effective numerical implementation of the proposed method is essential. In the present formulation, a very efficient parametric model reduction technique is considered. In particular, a model reduction technique based on substructure coupling for dynamic analysis is adopted [49, 50]. The method involves dividing the structure into a number of linear and nonlinear substructures, obtaining reduced-order models of the linear substructures and then assembling a reduced-order model of the entire structure. The dynamic behavior of the linear substructures is described by a set of dominant fixed-interface normal modes along with a set of interface constraint modes that account for the coupling at each interface where the substructures are connected [49]. Based on these modes, the corresponding reduced-order matrices can be derived.

While the use of reduced-order models alleviates part of the computational effort, their repetitive generation during the solution of the reliability problem can be computationally expensive due to the substantial computational overhead that arises at the substructure level. In this regard, an efficient model parametrization scheme is implemented. To this end, the division of the original model is guided by a parametrization scheme which assumes that the substructure matrices for each of the introduced linear substructures depend on only one of the model parameters. Based on this assumption, a direct parametrization of the reduced-order matrices associated with the linear substructures is obtained and, consequently, a drastic reduction in computational effort is achieved [50, 51]. In other words, the different quantities involved in the reduced-order model can be directly updated for different values of the model parameters $\boldsymbol{\theta}$. Thus, the potentially time-consuming step of computing the reduced-order matrices for different values of the model parameters is completely avoided. Moreover, the above formulation guarantees that the reduced-order model is based on the exact substructure modes for all values of the model parameters $\boldsymbol{\theta}$. The equation of motion of the reduced-order model together with the equation for the evolution of the set of variables $\boldsymbol{\tau}(t)$ can be integrated efficiently by any appropriate step-by-step integration scheme. A detailed derivation and formulation of the parametric model reduction technique can be found in [50].

Finally, it is noted that the use of parametric reduced-order models has also important implications from a practical viewpoint. In fact, the use of this technique opens the door to applications involving real structural dynamic systems and, therefore, the proposed implementation can contribute to the enhancement of the safety and reliability of practical engineering systems. Moreover, the consideration of surrogate models at the likelihood function level [40, 52] combined with the previous parametric model reduction technique can also be implemented to improve further the efficiency of the proposed scheme for solving the reliability problem. Such approach is currently under development and it will be reported in a future contribution (see Conclusions).

5. Examples

It is noted that validation calculations have shown that the different available BUS techniques and the proposed approach provide very similar results for the academic-type of problems presented in previous contributions. In this work, two examples comprising involved structural dynamic systems are presented. The first example comprises a benchmark system introduced in [20], which involves a linear ten-story shear building model subject to ground excitation. In this regard, this example allows to demonstrate the effectiveness of the proposed approach in predicting different types of responses as well as in identifying the spectral properties of the structural model. Additionally, a statistical performance analysis of alternative BUS approaches is provided for this example. On the other hand, the second example considers a realistic finite element model of a nonlinear three-dimensional bridge structure to demonstrate the applicability of the identification method in a complex structural system. In both examples, a large number of model parameters are considered. Additionally, it is assumed that noisy simulated acceleration data are available for updating purposes.

5.1. Example 1: Illustrative Problem

5.1.1. Identification Problem

The ten-story linear shear-building model shown in Figure 1, which has been borrowed from [20], is considered in this first example problem. The corresponding model class is characterized by the mass m_i, damping coefficient c_i, and stiffness parameter k_i for each story $i = 1, \ldots, 10$. The identification process is based on simulated acceleration data. In particular, the input ground acceleration history to generate the measurements, shown in Figure 2, corresponds to the El Centro ground-motion record. The input acceleration values have been scaled so that the peak ground acceleration is equal to 0.6 m/s^2. The measured response is simulated by first calculating the absolute acceleration response of the actual structure at the first and tenth floors. Thus, the number of observed degrees of freedom is $n_o = 2$. Then, a Gaussian discrete white noise sequence with standard deviation σ equal to 10% of the root-mean-square value of the corresponding acceleration time histories is added. Ten seconds of data with sampling interval $\Delta t = 0.01$ s are used, giving a total of $n_t = 1000$ time steps. The corresponding measurements are shown in Figure 2. The nominal model used to generate the measured data is defined in Table 1. This system may be interpreted as the actual or target structural system in a Bayesian model updating framework.

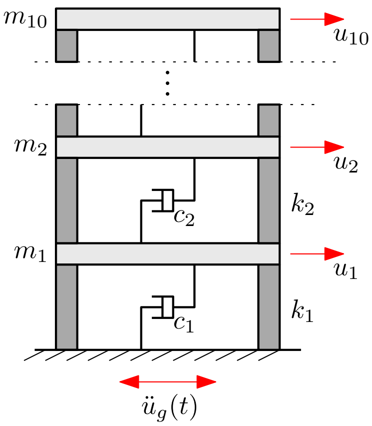

Figure 1: Ten-story linear shear building model.

Table 1: Target values of the model parameters. Example 1.

Parameter	Value	Parameter	Value	Parameter	Value
m_{1n}	1.92×10^4 kg	c_{1n}	7.70×10^4 Ns/m	k_{1n}	2.16×10^7 N/m
m_{2n}	1.97×10^4 kg	c_{2n}	7.78×10^4 Ns/m	k_{2n}	1.74×10^7 N/m
m_{3n}	1.95×10^4 kg	c_{3n}	7.86×10^4 Ns/m	k_{3n}	2.04×10^7 N/m
m_{4n}	2.06×10^4 kg	c_{4n}	7.28×10^4 Ns/m	k_{4n}	1.99×10^7 N/m
m_{5n}	2.05×10^4 kg	c_{5n}	7.19×10^4 Ns/m	k_{5n}	1.74×10^7 N/m
m_{6n}	1.98×10^4 kg	c_{6n}	7.37×10^4 Ns/m	k_{6n}	1.68×10^7 N/m
m_{7n}	1.94×10^4 kg	c_{7n}	7.10×10^4 Ns/m	k_{7n}	1.87×10^7 N/m
m_{8n}	2.06×10^4 kg	c_{8n}	7.11×10^4 Ns/m	k_{8n}	1.77×10^7 N/m
m_{9n}	1.90×10^4 kg	c_{9n}	6.90×10^4 Ns/m	k_{9n}	1.84×10^7 N/m
m_{10n}	2.01×10^4 kg	c_{10n}	7.57×10^4 Ns/m	k_{10n}	1.72×10^7 N/m
σ_n	3.74×10^{-2} m/s^2				

For identification purposes, 31 model parameters are selected. They correspond to the masses $m_i, i = 1, \ldots, 10$, damping coefficients $c_i, i = 1, \ldots, 10$, stiffness parameters $k_i, i = 1, \ldots, 10$, and the standard deviation of the prediction and measurement errors σ. It is noted that this problem can be regarded as high-dimensional from a Bayesian model updating point of view. Moreover, the mass, damping, and stiffness parameters can be uniformly scaled without changing the acceleration response of the structural model. For reference and comparison purposes, the properties of the actual structural system as well as the prior distribution of the uncertain parameters are defined as in [20]. The prior probability density functions of the model parameters m_i, c_i, and k_i, $i =$

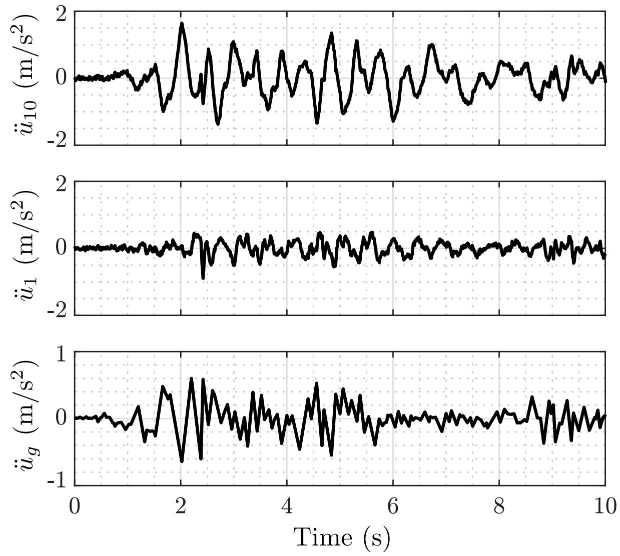

Figure 2: Input ground motion and measurement data. Example 1.

$1,\ldots,10$, correspond to Gaussian distributions with means equal to $\bar{m} = 2\times10^4$ kg, $\bar{c} = 6\times10^4$ Ns/m, $\bar{k} = 2\times10^7$ N/m, and coefficients of variation of 10%, 30%, and 30%, respectively. On the other hand, σ follows a lognormal distribution with median equal to 0.1 m/s^2 and a logarithmic standard deviation of 0.3, which leads to a coefficient of variation of approximately 30%. It is seen that the mean values of the uncertain parameters do not match the corresponding target or nominal values (exact values) of the model parameters (see Table 1).

For illustration purposes, the following user-defined parameters are considered for the numerical implementation of the proposed approach: number of samples per stage $N = 10000$, and conditional probability $p_0 = 0.1$. Note that a relatively large sample size is considered in order to focus on the effectiveness of the proposed scheme in a high-dimensional case and not on the effect of the number of samples per stage. In any case, additional validation calculations show that the number of samples per stage can be significantly reduced without affecting the performance of the identification process. Actually, around 2000 samples per stage are sufficient for the problem under consideration. Finally, due to the simplicity of the structural system, a reduced-order model is not considered in this example problem. Therefore, all analyses are performed using the original unreduced model.

5.1.2. Results

Figures 3, 4, 5 and 6 show the posterior marginal histograms associated with the mass, damping, stiffness and standard deviation parameters, respectively. For presentation purposes, the model parameters have been normalized with respect to their target values (see Table 1) as $\hat{\theta}_i = m_i/m_{in}, i = 1, ..., 10$, $\hat{\theta}_i = c_{i-10}/c_{(i-10)n}, i = 11, ..., 20$, $\hat{\theta}_i = k_{i-20}/k_{(i-20)n}, i = 21, ..., 30$, and $\hat{\theta}_{31} = \sigma/\sigma_n$. It is seen that the posterior samples tend to be concentrated relatively close to the target values, i.e., $\hat{\theta}_i = 1$, $i = 1, \dots, 31$. Compared with the prior uncertainty in the structural model parameters, the posterior uncertainty is significantly reduced since the data provide relevant information about these parameters. The same result is obtained for the parameter associated with the standard deviation of the prediction and measurement errors, σ, as shown in Figure 6.

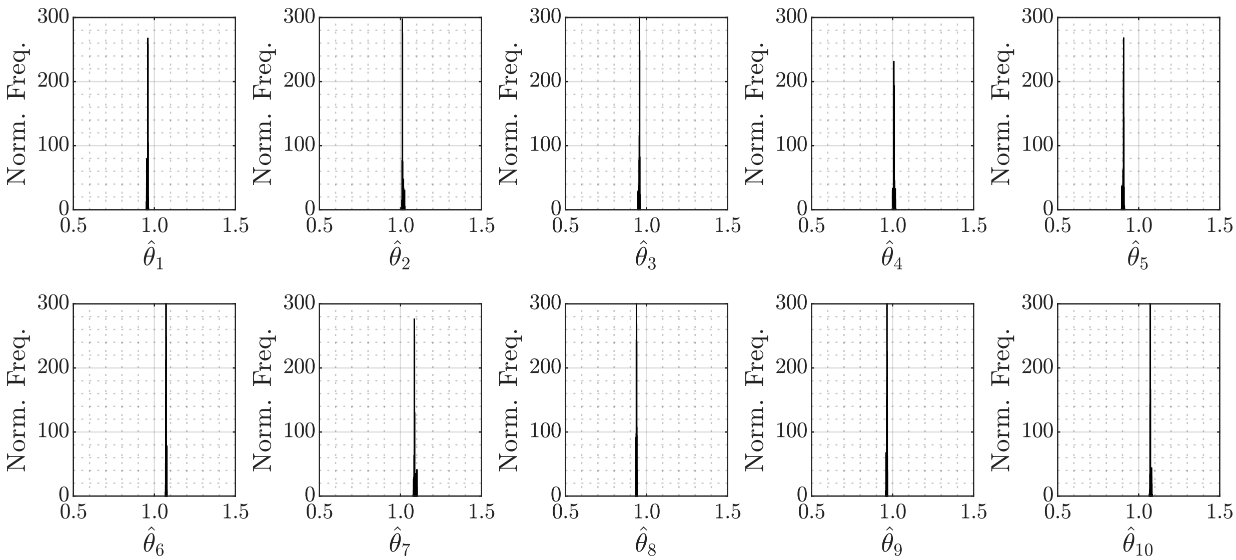

Figure 3: Posterior marginal histograms corresponding to the normalized mass parameters.

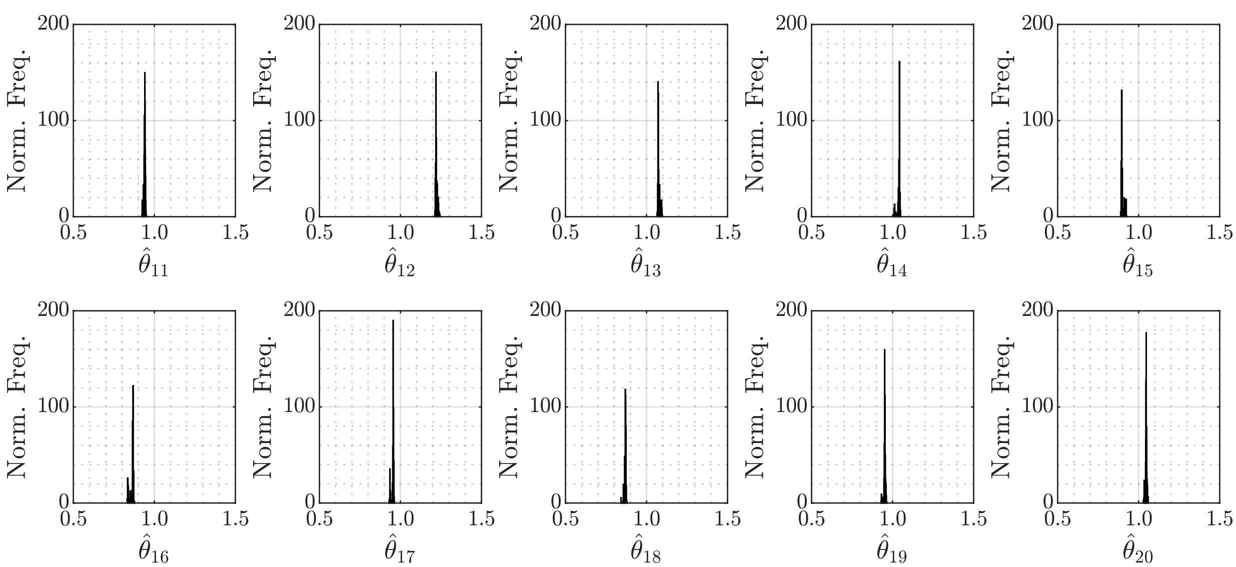

Figure 4: Posterior marginal histograms corresponding to the normalized damping parameters.

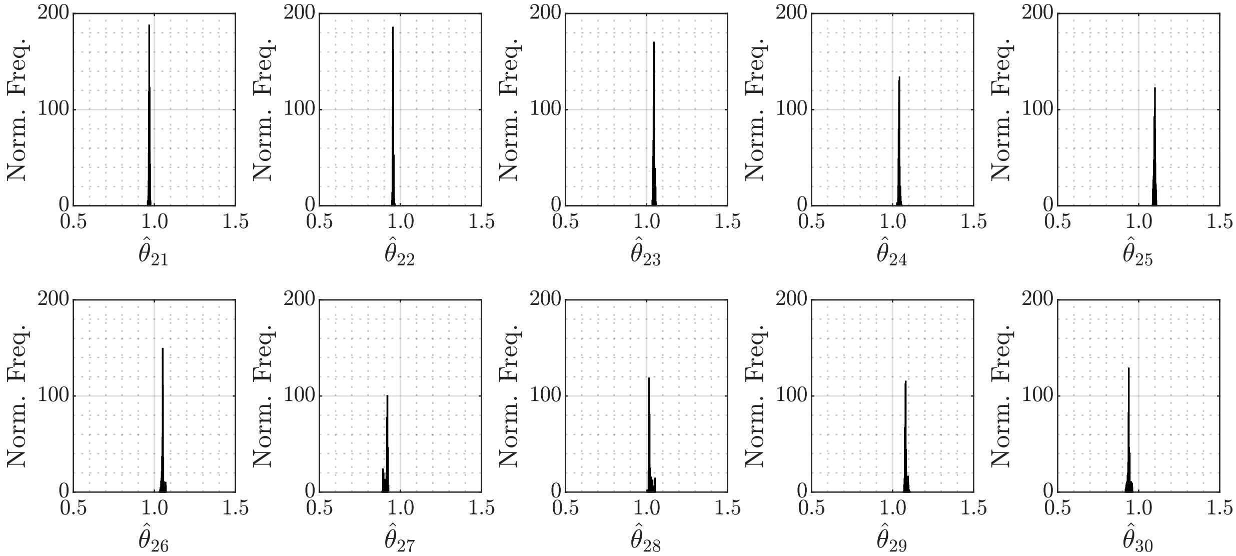

Figure 5: Posterior marginal histograms corresponding to the normalized stiffness parameters.

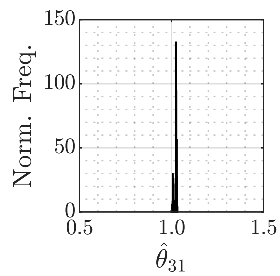

Figure 6: Posterior marginal histogram corresponding to the normalized standard deviation of the prediction and measurement errors.

The posterior mean values of the normalized variables are shown in Table 2. It is observed that there are larger deviations between the target and posterior mean values of the damping parameters than of the mass and stiffness parameters. In fact, this is expected from a structural viewpoint since the modal contributions to the response are more sensitive to the mass and stiffness than to the damping. The corresponding estimation error is less than 10% for the mass and stiffness parameters and less than 20% for the damping parameters. These deviations from the target values are reasonably small and, as shown in what follows, they marginally affect the quality of the identification results in terms of the updated spectral properties of the structural system and of the updated response prediction.

Based on the information from the posterior samples of the model parameters, the corresponding spectral properties of the structural model can be computed and compared with the exact values. In Table 3, the sample mean (with sample c.o.v. inside the parenthesis) of the natural

Table 2: Posterior mean values of the normalized parameters. Example 1.

Parameter	Value	Parameter	Value	Parameter	Value
$\hat{\theta}_1$	0.958	$\hat{\theta}_{11}$	0.940	$\hat{\theta}_{21}$	0.968
$\hat{\theta}_2$	1.014	$\hat{\theta}_{12}$	1.192	$\hat{\theta}_{22}$	0.955
$\hat{\theta}_3$	0.956	$\hat{\theta}_{13}$	1.076	$\hat{\theta}_{23}$	1.045
$\hat{\theta}_4$	1.008	$\hat{\theta}_{14}$	1.038	$\hat{\theta}_{24}$	1.041
$\hat{\theta}_5$	0.906	$\hat{\theta}_{15}$	0.900	$\hat{\theta}_{25}$	1.098
$\hat{\theta}_6$	1.072	$\hat{\theta}_{16}$	0.862	$\hat{\theta}_{26}$	1.052
$\hat{\theta}_7$	1.088	$\hat{\theta}_{17}$	0.953	$\hat{\theta}_{27}$	0.914
$\hat{\theta}_8$	0.938	$\hat{\theta}_{18}$	0.868	$\hat{\theta}_{28}$	1.022
$\hat{\theta}_9$	0.965	$\hat{\theta}_{19}$	0.951	$\hat{\theta}_{29}$	1.081
$\hat{\theta}_{10}$	1.073	$\hat{\theta}_{20}$	1.046	$\hat{\theta}_{30}$	0.939
				$\hat{\theta}_{31}$	1.022

frequency and damping ratio for each mode along with the target values of the natural frequency and damping ratio are shown. Note that the model has nonclassical damping and, therefore, it has complex modes. It is observed that the relative errors are quite small. Actually, the maximum relative error is around 3%, which is observed for the higher-order modes. Moreover, the estimates of the first modes are much better than those of the higher-order modes. In fact, the maximum relative error for the five first modes is below 0.5%. This is because only the first complex modes of the model are excited significantly by the ground acceleration, so it is this information from the first modes that is utilized in estimating the model parameters.

To illustrate the predictive power of the previous identification scheme, the exact time histories of the displacement, drift response, and total acceleration of some unobserved floors are compared with the corresponding posterior predictions in Figures 7, 8, and 9, respectively. The solid-black line shows the exact values of the response and the dashed-red line shows the corresponding posterior mean prediction. In addition, the posterior 95%-confidence interval, denoted by dotted-blue lines, is also presented in the figures. The curves for the exact and the mean responses are indistinguishable. Likewise, the 95%-confidence interval is almost indistinguishable from the other two curves. Thus, the Bayesian analysis is able to provide a high-quality updated prediction of the response even at unobserved degrees of freedom.

Table 3: Natural frequencies and damping ratios associated with the target parameter values and with the posterior distribution of the model parameters.

	Target model		Bayesian updating			
Complex mode	Natural frequency (Hz)	Damping ratio (%)	Natural frequency (Hz)		Damping ratio (%)	
1	0.7343	0.92	0.7345	(0.04%)	0.94	(0.21%)
2	2.1568	2.71	2.1562	(0.01%)	2.67	(0.32%)
3	3.5585	4.45	3.5603	(0.05%)	4.20	(0.33%)
4	4.8896	6.03	4.9027	(0.09%)	6.05	(0.44%)
5	6.0470	7.65	6.0526	(0.11%)	7.43	(0.42%)
6	7.1032	9.11	7.2022	(0.11%)	9.06	(0.22%)
7	8.0466	10.14	7.9530	(0.07%)	10.52	(0.28%)
8	8.6097	11.12	8.8519	(0.08%)	11.05	(0.22%)
9	9.2989	11.58	9.3704	(0.15%)	10.77	(0.55%)
10	9.6355	11.92	9.8938	(0.10%)	12.11	(0.31%)

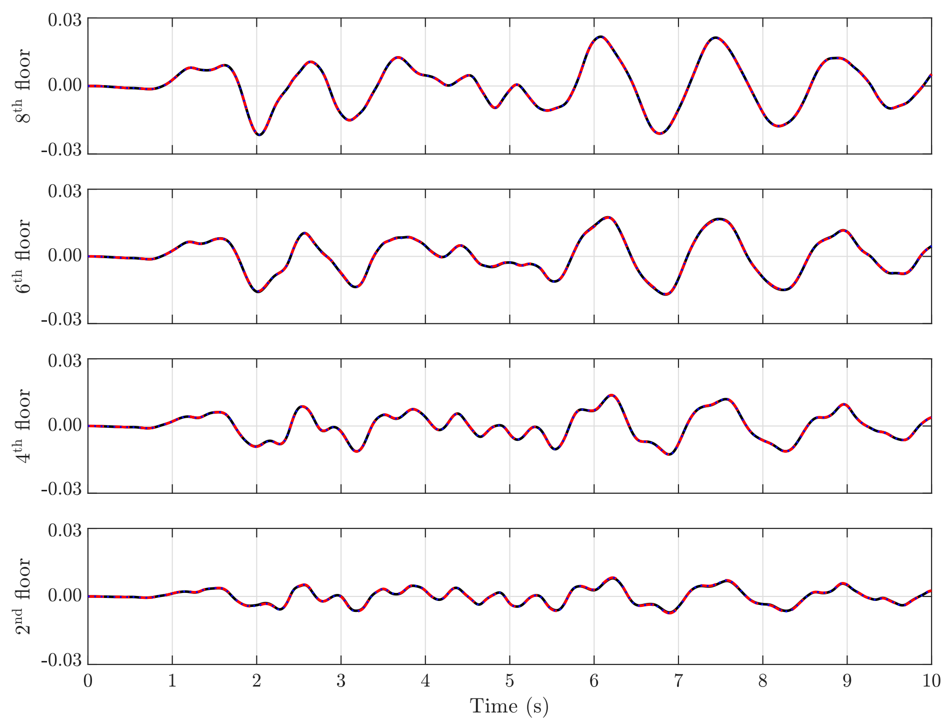

Figure 7: Exact value (solid-black), posterior mean prediction (dashed-red), and posterior 95%-confidence interval (dotted-blue) of the displacement (in m) at floors 2, 4, 6 and 8.

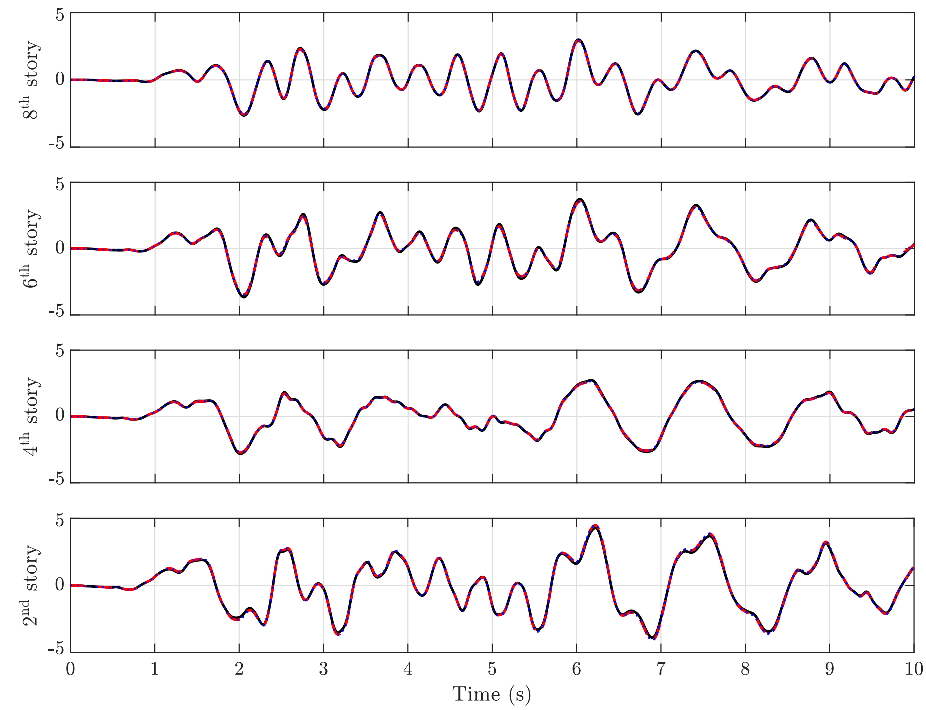

Figure 8: Exact value (solid-black), posterior mean prediction (dashed-red), and posterior 95%-confidence interval (dotted-blue) of the drift response (in mm) at floors 2, 4, 6 and 8.

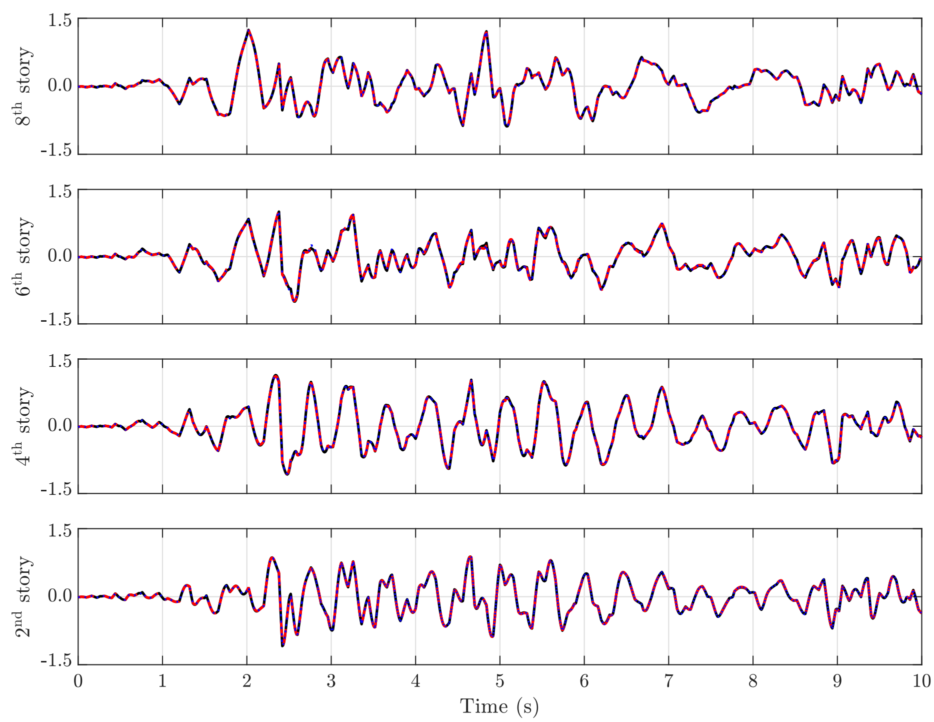

Figure 9: Exact value (solid-black), posterior mean prediction (dashed-red), and posterior 95%-confidence interval (dotted-blue) of the total acceleration (in m/s^2) at floors 2, 4, 6 and 8.

5.1.3. Performance of Proposed and Alternative BUS Approaches

To study the performance of available BUS approaches, a statistical analysis of the log-evidence estimates is carried out. This quantity is selected since its computation involves the likelihood multiplier and the failure event of the equivalent reliability problem, two key aspects of BUS formulations. Along with the proposed approach, the following methods have been considered: adaptive driving variable-based BUS (A-BUS) [32], inner reliability problem-based BUS (I-BUS) [31], standard BUS with a priori definition of the likelihood multiplier (S-BUS) [26], and postprocessing-based BUS (P-BUS) [30]. Rejection sampling has been implemented in P-BUS with a target number of failure samples equal to 1000. The rest of the methods consider subset simulation with $N = 10000$ samples per stage and conditional probability $p_0 = 0.1$. For each method, 30 independent runs are performed. Two cases for the tolerance value associated with the stopping criterion of I-BUS are implemented, i.e., $P_{\text{tol}} = 10^{-8}$ and $P_{\text{tol}} = 10^{-3}$. For comparison and reference purposes, the maximum values for $\ln(c^{-1})$ obtained in these two cases are considered in S-BUS. Additionally, P-BUS considers the maximum value of $\ln(c^{-1})$ obtained for I-BUS with $P_{\text{tol}} = 10^{-3}$ in order to illustrate the effect of the postprocessing step on the quality of the results.

Table 4: Statistical performance across 30 independent runs of different BUS methods. Example 1.

Method	User-defined parameter	Number of function calls	Average log-evidence	Maximum $\ln(c^{-1})$
This work	–	4.2×10^5	3.58×10^3	3.78×10^3
A-BUS [32]	–	4.4×10^5	3.59×10^3	3.78×10^3
I-BUS [31]	$P_{\text{tol}} = 10^{-8}$	5.1×10^5	3.22×10^3	3.38×10^3
I-BUS [31]	$P_{\text{tol}} = 10^{-3}$	1.5×10^5	2.34×10^3	2.38×10^3
S-BUS [26]	$\ln(c^{-1}) = 3.38 \times 10^3$	1.1×10^5	3.36×10^3	–
S-BUS [26]	$\ln(c^{-1}) = 2.38 \times 10^3$	4.0×10^4	2.37×10^3	–
P-BUS [30]	$\ln(c^{-1}) = 2.38 \times 10^3$	1.2×10^6	3.03×10^3	–

Table 4 presents the average number of function calls, average log-evidence and maximum values for $\ln(c^{-1})$ obtained by the different methods across 30 independent runs. Note that the maximum values for $\ln(c^{-1})$ are not given for S-BUS and P-BUS, since the likelihood multiplier is defined a priori in these methods. In addition, the user-defined parameters required by the different methods are also presented in the table. Several observations can be made from these results. First, the evidence tends to be more underestimated for smaller values of $\ln(c^{-1})$. Such a behavior is consistent with the relationship between the evidence estimate and the likelihood multiplier, as discussed in previous contributions [30, 31]. Further, it illustrates the significant effect that this parameter can have on the performance of BUS formulations. Second, the maximum values for $\ln(c^{-1})$ obtained by I-BUS are smaller than those computed by A-BUS and the proposed approach. Third, the evidence estimates obtained by S-BUS ($\ln(c^{-1}) = 2.38 \times 10^3$) and I-BUS ($P_{tol} = 10^{-3}$) are similar, as expected. Analogous results are observed in the cases of S-BUS ($\ln(c^{-1}) = 3.38\times10^3$) and I-BUS ($P_{tol} = 10^{-8}$). At the same time, the computational efforts are higher in I-BUS due to the iterative solution of the inner reliability problem. Fourth, the average log-evidence estimates of P-BUS are higher than of S-BUS for $\ln(c^{-1}) = 2.38 \times 10^3$. Thus, the postprocessing strategy proposed in [30] appears to be effective in improving the quality of the evidence estimates for this example. Fifth, the computational efforts of P-BUS, which involves the use of rejection sampling, are around two orders of magnitude higher than of S-BUS for $\ln(c^{-1}) = 2.38 \times 10^3$. This shows an additional strength of adopting subset simulation as reliability analysis technique, since it can efficiently handle small failure probabilities. In this regard, the adaptation and evaluation of alternative structural reliability methods for Bayesian model updating represents an interesting research venue. Finally, the performances of the proposed approach and A-BUS are very similar, which is reasonable since both methods select the final likelihood multiplier based on the maximum observed likelihood value. Nonetheless, as already pointed out, the formulation presented in this work is simpler since there is no need to redefine the driving variable function at each iteration. As a result, only minimal modifications to the standard subset simulation algorithm are required by the proposed approach. Overall, the proposed updating technique can be regarded as a viable alternative BUS approach which is attractive for practical applications due to the simplicity of both its formulation and implementation.

5.2. Example 2: Application Problem

The objective of this application is to evaluate the performance of the proposed approach in an identification problem involving a realistic nonlinear structural model with multiple uncertain parameters and noisy seismic response data.

5.2.1. Description of Structural Model

A three-dimensional bridge finite element model with more than 10000 degrees of freedom is considered as application problem. The bridge model, which has been taken from [53], is shown in Figure 10. It is curved in plan and has a total length of 119.0 m with five spans of lengths equal to 24.0 m, 20.0 m, 23.0 m, 25.0 m, and 27.0 m. Four piers of 8.0 m height support the girder monolithically, where each pier is founded on an array of four piles of 35.0 m height. The piers and piles are modeled as column elements of circular cross-section with diameters of 1.6 m and 0.6 m, respectively. In addition, the deck cross section is a box girder modeled by beam and shell elements. The deck girder rests on each abutment through two sliding bearings which are composed of an upper steel plate with a housing cap for the slider, a bottom plate with a concave semi-spherical stainless steel surface, and a steel slider.

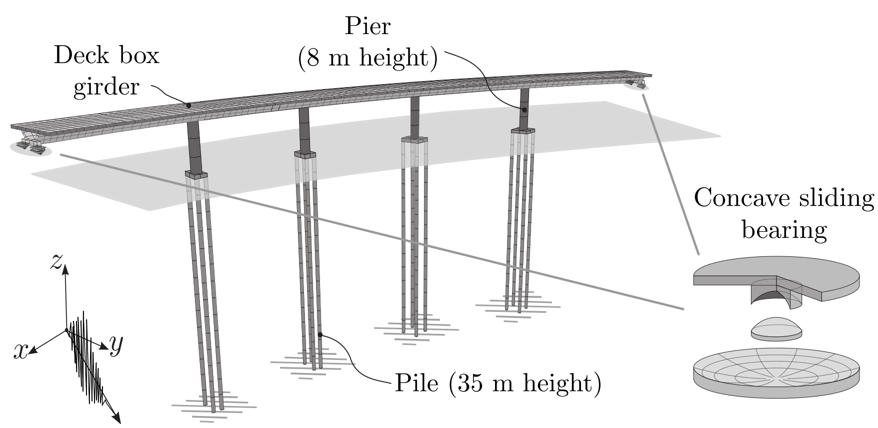

Figure 10: Isometric view of the finite element model of the bridge structure with friction-based devices at the abutments.

An experimentally validated model that takes into account the main sources of performance degradation that friction-based devices experience during seismic events is implemented in the structural model [54]. The major effects related to the frictional performance of these devices include: the load effect related to the reduction of the friction coefficient as the vertical load increases, the velocity effect that takes into account the variation of the friction coefficient with the velocity of motion, and the cycling effect which is responsible for the degradation of friction characteristics due to temperature rise. The reader is referred to [54, 55, 56] for a detailed description and implementation of the experimentally validated model. For illustration purposes, a typical displacement-restoring force curve of these devices is shown in Figure 11.

The interaction between the piles and the soil is modeled by a series of translational springs

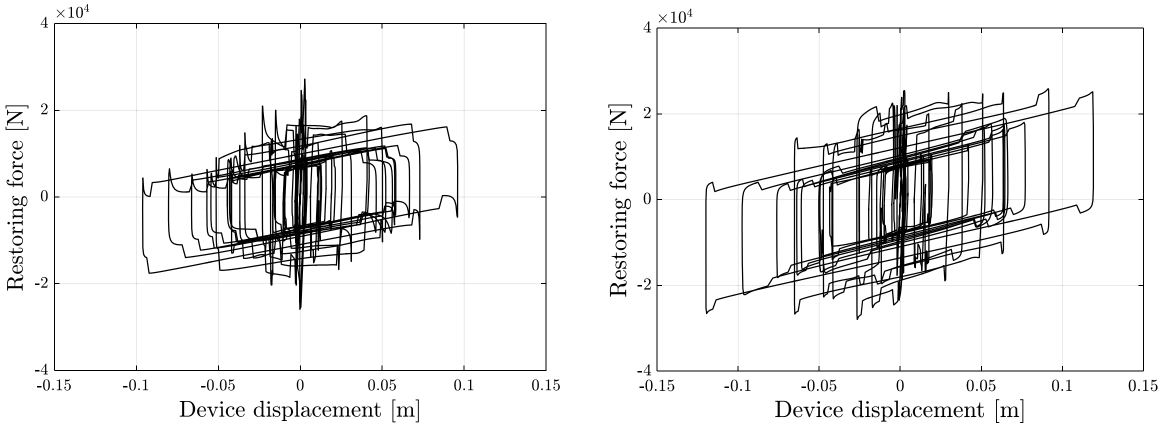

Figure 11: Typical displacement-restoring force curve of the sliding bearing. Left: x direction. Right: y direction.

along the height of the piles with a nominal linear stiffness profile varying from 11200 T/m at the bottom of the piles to 560 T/m at the surface. The net effect of these springs is to increase the translational stiffness in the x and y direction of the column elements that model the piles. Nominal material properties of the structural model have been assumed as follows: Young's modulus $E = 2.0 \times 10^{10}$ N/m^2; Poisson ratio $\nu = 0.2$, and mass density $\rho = 2500$ kg/m^3. A 3% of critical damping is added to the model. It is assumed that the structural components such as the piers, piles and the deck girder remain linear during the analysis while the nonlinearities are localized in the sliding bearings response.

5.2.2. Parametric Reduced-Order Model

In order to improve the numerical efficiency of the updating procedure, a parametric reduced-order model of the bridge structure is implemented. In particular, the structural model is subdivided into sixteen linear substructures and two nonlinear substructures as shown in Figure 12. Substructures $S_i, i = 1, \ldots, 5$ are related to the five spans of the bridge deck, substructures $S_i, i = 6, \ldots, 9$ are associated with the four piers, while substructures $S_i, i = 10, \ldots, 13$ comprise the four arrays of piles and the corresponding pile footings. In addition, the translational springs that model the interaction between the piles and the soil are included in three substructures, i.e, $S_i, i = 14, \ldots, 16$ as shown in the figure. Finally, the sliding bearings at each abutment are considered in substructures $S_i, i = 17, 18$. Thus, substructures $S_i, i = 1, \ldots, 16$ are linear while S_{17} and S_{18} are nonlinear.

The reduced-order model is characterized in terms of interface constraint modes and a set of dominant fixed-interface normal modes (see Section 4.2). In this regard, 400 interface degrees

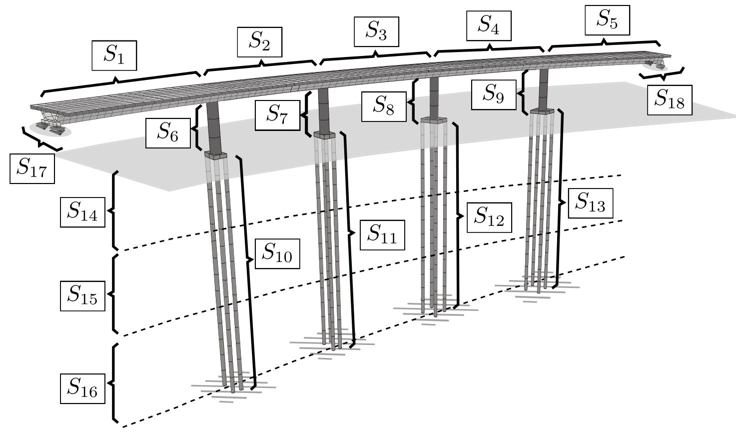

Figure 12: Linear and nonlinear substructures of the finite element model.

of freedom are present at the interfaces of the finite element model. Additionally, five fixed-interface normal modes are kept for each substructure $S_i, i = 1, \dots, 5$, three for each substructure $S_i, i = 6, \dots, 9$, and three for each substructure $S_i, i = 10, \dots, 13$. Note that substructures $S_i, i = 14, 15, 16$ compress interface degrees of freedom only. As a result, the number of generalized coordinates is equal to 449, which corresponds to a reduction of more than 95% with respect to the total number of degrees of freedom. Thus, the reduced-order model provides a significant dimension reduction with respect to the original unreduced finite element model. Validation calculations show that the selected reduced-order model is able to capture the dynamics of the unreduced model with great accuracy. In this regard, Figure 13 shows a 3-D representation of the matrix of modal assurance criterion (MAC) values [57] between the 10 first modal vectors computed from the full finite element model and the reduced-order model. For comparison purposes, only the linear components of the undamped structural model are considered in the computation of mode shapes and natural frequencies. It is seen that the off-diagonal terms are almost zero and, hence, both models are consistent in terms of their mode shapes. Moreover, additional computations show that the errors for the ten lowest natural frequencies fall bellow 0.5%. The comparison in terms of the ten lowest-order modes seems reasonable since the contribution of higher-order modes in the dynamic response of the model is negligible in this case. From the practical point of view it is important to note that the selection of the fixed-interface modes per substructure, necessary to achieve a prescribed accuracy, is done offline, before the updating process takes place [50].

Eighteen parameters associated with structural properties of different sections of the structure are considered to characterize the finite element model, which are denoted as $\zeta_i, i = 1, \dots, 18$.

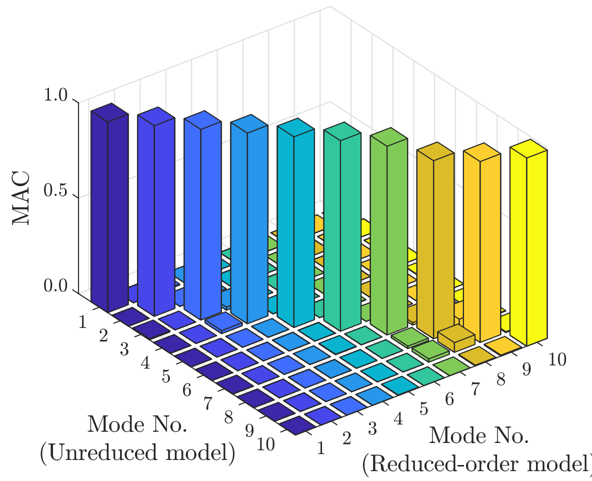

Figure 13: Modal assurance criterion (MAC) values between the mode shapes associated with the full and reduced-order models.

They are related to the modulus of elasticity of each span of the bridge deck ($\zeta_i, i = 1, \ldots, 5$), the modulus of elasticity of each pier ($\zeta_i, i = 6, \ldots, 9$), the modulus of elasticity of each pile ($\zeta_i, i = 10, \ldots, 13$), the stiffness constants of the springs along the height of the piles ($\zeta_i, i = 14, 15, 16$), and the friction coefficients of the sliding bearings at the abutments ($\zeta_i, i = 17, 18$). Thus, based on the subdivision of the finite element model, it is seen that each substructure is associated with a single parameter. Furthermore, the parameters are defined such that $\zeta_i = 1, i = 1, \ldots, 18$, corresponds to the nominal or reference values for the different structural properties. Using this information, the reduced-order matrices associated with the linear substructures can be efficiently parametrized as indicated in Section 4.2.

Numerical validations indicate that the implementation of the parametric reduced-order model allows to obtain a speedup factor of more than 10 for the computation of the structural response in this case. In this context, the speedup factor corresponds to the ratio between the execution time by considering the full finite element model and the proposed parametric reduced-order model. Since most of the computational efforts involved in the updating procedure are associated with the solution of the equation of motion for different values of the uncertain parameters, the parametrization scheme under consideration provides significant computational savings for the overall identification process.

5.2.3. Simulated Data

Synthetically generated measurements are considered for identification purposes. The corresponding ground excitation is the El Centro ground-motion record, which is applied at 50° with respect to the x axis (see Figure 10) and has been scaled to a peak ground acceleration of 5 m/s^2. Acceleration responses along the x and y directions at the midpoints of the five spans of the deck are considered for identification purposes. In addition, 20 s of response with a sampling interval of $\Delta t = 0.01$ s are considered. Thus, the identification data comprise $n_o = 10$ observed degrees of freedom and $n_t = 2000$ time steps. As in the previous example, the measurements are generated by contaminating the actual acceleration responses with a Gaussian discrete white noise sequence whose standard deviation is equal to 10% of the root-mean-square value of the responses. Table 5 shows the actual values of the parameters that are used to generate the measured data, where $\zeta_{in}, i = 1, \dots, 18$ are the actual parameter values associated with the different substructures and σ_n is the actual standard deviation (in m/s^2) of the prediction and measurement errors. For illustration purposes, the input ground motion as well as the measurements at the midpoint of the bridge's deck along the x and y directions are presented in Figure 14.

Table 5: Actual values of the model parameters. Example 2.

Parameter	Value	Parameter	Value	Parameter	Value
ζ_{1n}	0.87	ζ_{7n}	0.98	ζ_{13n}	1.06
ζ_{2n}	1.07	ζ_{8n}	1.14	ζ_{14n}	1.05
ζ_{3n}	0.93	ζ_{9n}	0.94	ζ_{15n}	0.90
ζ_{4n}	0.98	ζ_{10n}	1.06	ζ_{16n}	0.89
ζ_{5n}	1.01	ζ_{11n}	0.95	ζ_{17n}	1.12
ζ_{6n}	1.13	ζ_{12n}	1.04	ζ_{18n}	0.90
				σ_n	8.01×10^{-2}

5.2.4. Results

For identification purposes, all structural parameters are considered as uncertain, i.e., $\theta_i = \zeta_i,\ i = 1, \dots, 18$ (see Section 5.2.2). In addition, the standard deviation of the prediction and measurement errors is also considered in the set of uncertain parameters as $\theta_{19} = \sigma$. Thus, the Bayesian model updating problem comprises a total of $n_\theta = 19$ parameters to be identified. Note that this is a high-dimensional problem from the identification point of view. The prior probability density function of each structural parameter $\theta_i, i = 1, \dots, 18$, is taken as uniform over the interval $[0.5, 1.5]$, while the prior distribution of θ_{19} is lognormal with median equal to 0.1

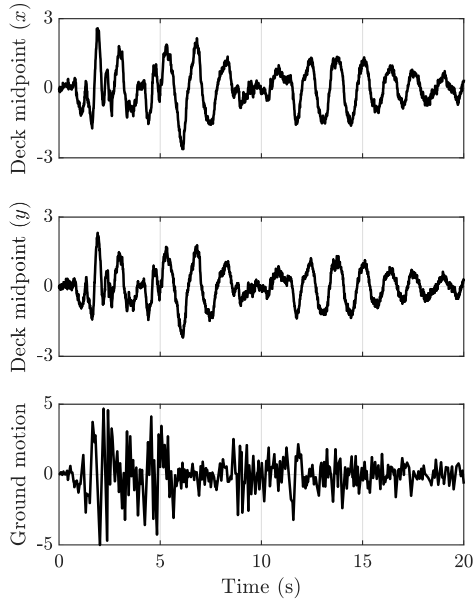

Figure 14: Input ground motion and acceleration measurements (in m/s^2) at the midpoint of the deck's central span. Example 2.

m/s^2 and a logarithmic standard deviation of 0.3. According to this definition, the prior means of the uncertain parameters differ from their corresponding target values.

In the context of the proposed identification scheme, a sample size equal to $N = 2000$ and a conditional probability of $p_0 = 0.1$ are considered. Table 6 shows the posterior mean values of the uncertain parameters obtained at the end of the sampling process. For presentation purposes, the parameters haven been normalized by their target values (see Table 5) as $\hat{\theta}_i = \theta_i/\zeta_{in}, i = 1, \ldots, 18$ and $\hat{\theta}_{19} = \theta_{19}/\sigma_n$. Relatively small differences with respect to the target values are obtained for the parameters associated with the deck (θ_i, $i = 1, \ldots, 5$), bearings (θ_{17} and θ_{18}), and standard deviation of the prediction errors (θ_{19}). Validation calculations suggest that these parameters have a significant effect on the system response. On the other hand, deviations with respect to the target values are observed for the parameters associated with the piers ($\theta_i, i = 6, \ldots, 9$) and piles ($\theta_i, i = 10, \ldots, 13$). This can be attributed to the interaction between these parameters. In terms of the substructures associated with the soil springs, it is seen that the posterior mean of the parameter associated with the superficial soil layer (θ_{14}) matches its target value, whereas the posterior mean estimates corresponding to the lower soil layers (θ_{15} and θ_{16}) present larger deviations with respect to their target values. This is reasonable from the engineering viewpoint and can be presumably attributed to a higher sensitivity of the deck acceleration response with respect to the stiffness of the superficial soil layer (θ_{14}), as it affects the horizontal stiffness of the entire foundation system to a greater extent. It is noted that similar results are obtained when considering different runs of the proposed approach.

Table 6: Posterior mean values of the normalized model parameters. Example 2.

Parameter	Value	Parameter	Value
$\hat{\theta}_1$	0.956	$\hat{\theta}_{11}$	1.247
$\hat{\theta}_2$	1.011	$\hat{\theta}_{12}$	0.751
$\hat{\theta}_3$	0.982	$\hat{\theta}_{13}$	1.192
$\hat{\theta}_4$	1.029	$\hat{\theta}_{14}$	1.003
$\hat{\theta}_5$	1.043	$\hat{\theta}_{15}$	1.322
$\hat{\theta}_6$	1.146	$\hat{\theta}_{16}$	0.894
$\hat{\theta}_7$	1.149	$\hat{\theta}_{17}$	1.003
$\hat{\theta}_8$	0.811	$\hat{\theta}_{18}$	0.996
$\hat{\theta}_9$	0.843	$\hat{\theta}_{19}$	1.008
$\hat{\theta}_{10}$	0.891		

The predictive capabilities of the proposed method in terms of the system response are shown in Figure 15. This figure presents the target responses (solid-black line) of the horizontal displacements at the abutments, as well as the mean predictions (dotted-red line) and the 95%-confidence intervals (grey area) associated with the prior (left plots) and posterior (right plots) distributions. Note that the prior mean predictions present some deviations with respect to the target responses and, in addition, the uncertainty in such predictions is considerable. However, the incorporation of available measurement data allows to improve the predictive capabilities of the model class. Recall that, according to Eq. (5), the likelihood function is defined in terms of a measure-of-fit function between the measured responses and the model prediction. Hence, the objective and goal of the proposed method is to find a set of parameters that provides high-quality updated predictions of the response. In this regard, the different lines in the right plots, which are associated with the posterior distribution, are indistinguishable between each other. That is, the target and expected responses agree very well and, moreover, the uncertainty in the response prediction is significantly reduced. Thus, the results indicate that the proposed approach is able to update the information on the system response in an effective manner for this case.

Figure 16 shows the evolution of the threshold level, v^{th}, during the different stages of subset

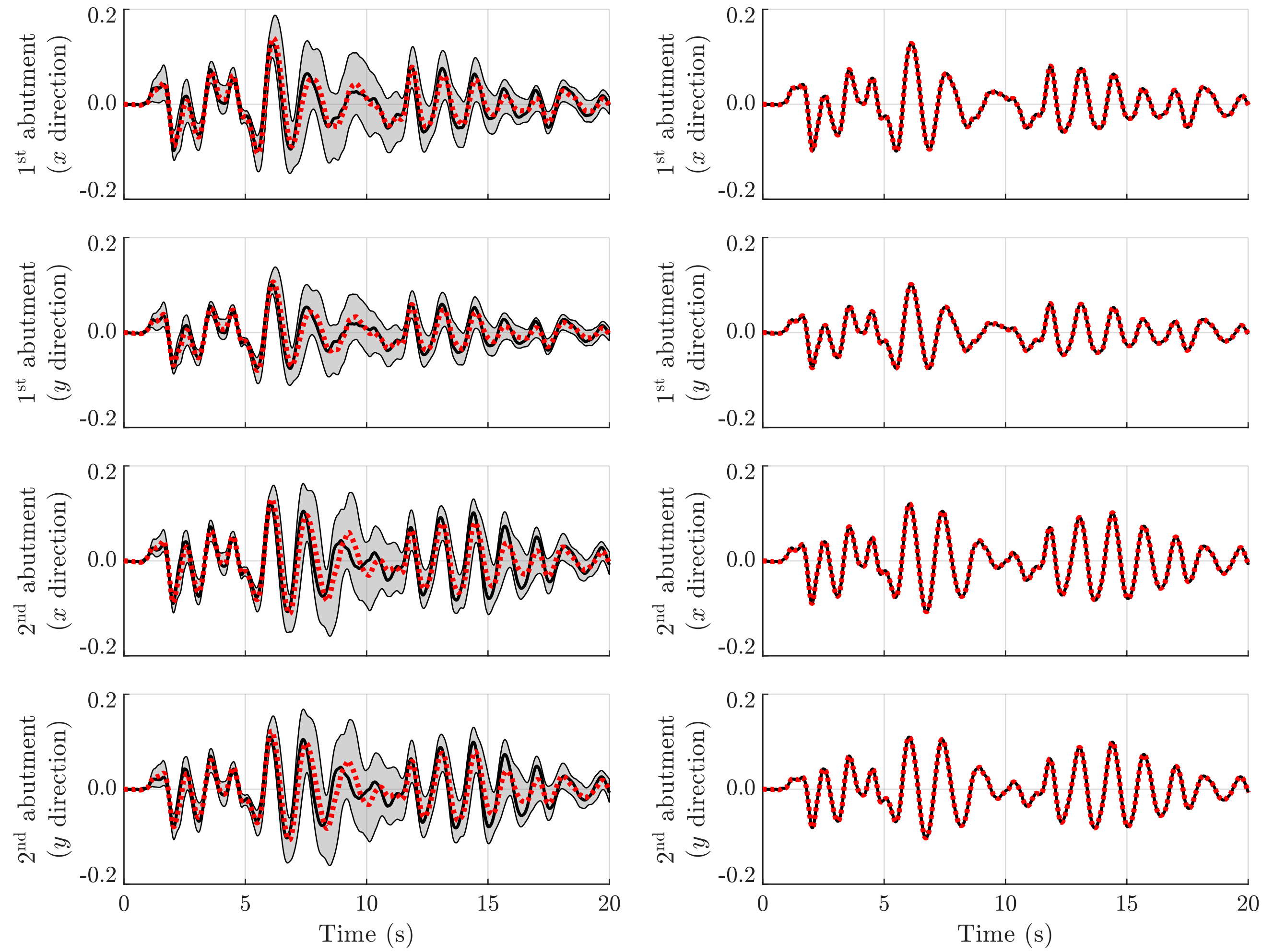

Figure 15: Target response (solid-black line), mean predictions (dotted-red line), and 95%-confidence intervals (grey area) of the horizontal displacements at the abutments. Left: Prior distribution. Right: Posterior distribution. Example 2.

simulation. Recall that this variable corresponds to the maximum log-likelihood value observed until the current stage. The results show that the method requires 20 stages to meet the stopping criterion. Nonetheless, the threshold level is stabilized roughly after 15 stages and it marginally increases during the final simulation levels. In this regard, the simulation process can be potentially stopped during an intermediate stage to retrieve samples that follow a truncated version of the posterior distribution [30]. However, the validity of such approach is problem-dependent and, therefore, the accuracy of the corresponding results must be assessed for each application. Finally, Table 7 shows the log-evidence estimates obtained across ten independent runs of the proposed simulation scheme. Rather stable estimates are observed in this case. Thus, the method is able to provide robust evidence estimates for this high-dimensional model updating problem involving a complex structural model equipped with nonlinear devices.

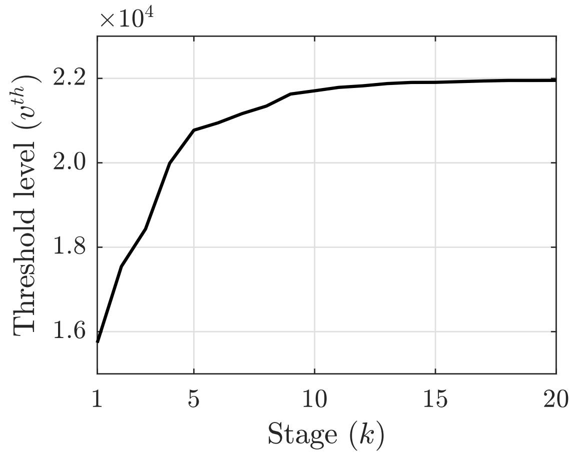

Figure 16: Evolution of threshold level. Example 2.

Table 7: Log-evidence estimates obtained in ten independent runs of the proposed scheme. Example 2.

Run No.	Log-evidence	Run No.	Log-evidence
1	2.19×10^4	6	2.19×10^4
2	2.18×10^4	7	2.19×10^4
3	2.19×10^4	8	2.20×10^4
4	2.18×10^4	9	2.19×10^4
5	2.19×10^4	10	2.19×10^4

6. Conclusions

An effective numerical implementation for Bayesian model updating of structural dynamic systems involving multiple uncertain parameters and measured responses has been presented in this contribution. The proposed scheme is based on the use of structural reliability methods, where samples following the posterior distribution are obtained as failure samples corresponding to an equivalent reliability problem. In this framework, an estimate of the evidence is obtained as a byproduct of the sampling process. Subset simulation, a well known and widely applied stochastic simulation technique, is adopted to generate the required failure samples. A strategy that adaptively determines the threshold level beyond which the corresponding failure samples follow the posterior distribution is implemented. Furthermore, only minimum modifications to the standard subset simulation algorithm are needed and no prior knowledge about the maximum likelihood value is required. These features are beneficial from a practical viewpoint. For an efficient numerical implementation of the proposed approach, an effective parametric reduced-order model formulation based on substructure coupling for dynamic analysis is considered. The resulting approach represents an alternative Bayesian identification technique based on structural reliability methods which provides an effective treatment of the maximum likelihood value while maintaining simplicity in its formulation and implementation.

Two examples have been studied to demonstrate the effectiveness and robustness of the proposed implementation, including a realistic model of a bridge structure equipped with nonlinear devices. Noisy acceleration measurements are synthetically generated for identification purposes. The important modal properties and the system response prediction are properly updated in both cases. In general, relatively few stages in the framework of subset simulation are required to stabilize the threshold level. This indicates the validity of the proposed method, since it is able to explore effectively the important region of the likelihood function. Similarly, the evidence estimates obtained across independent runs of the approach are rather stable for the problems analyzed in this contribution. Finally, the parametric reduced-order model strategy allows substantial computational savings without compromising the quality of the identification results. Overall, the results suggest that the proposed implementation is an effective and direct tool to address Bayesian model updating problems involving complex structural dynamic models, measured response data and high-dimensional parameter spaces. Furthermore, these developments open the door to applications involving real structural dynamic systems, which can in turn contribute to enhance the safety, reliability and life-cycle management of existing structures.

Future research efforts involve the integration of surrogate models at the likelihood function level, which can allow additional computational savings by reducing the number of calls to the parametric reduced-order model. Another research direction corresponds to the assessment of alternative techniques for generating the conditional samples at each simulation level, such as the implementation of different proposal distributions or methods based on auxiliary dynamic systems. Further, a thorough comparison between alternative BUS formulations as well as between different structural reliability methods, in the framework of complex structural dynamic systems, is an interesting and important topic for future work. Also, the characterization of complex posterior distributions associated with the identification of involved structural dynamic systems with multiple uncertain parameters as well as the consideration of measured response data, i.e., field data, are additional aspects of practical relevance. Finally, the assessment of the proposed scheme for Bayesian model class selection and model averaging problems, i.e., updated prediction of response quantities based on different model classes, in the context of high-dimensional parameter spaces is an additional subject for future research. Some of these topics are currently under consideration.

Acknowledgments

The research reported here was partially supported by ANID (National Agency for Research and Development, Chile) under its program FONDECYT, grant number 1200087. Also, this research has been supported by ANID and DAAD (German Academic Exchange Service) under CONICYT-PFCHA/Doctorado Acuerdo Bilateral DAAD Becas Chile/2018-62180007. These supports are gratefully acknowledged by the authors.

References

References

[1] Q. Huang, P. Gardoni, and S. Hurlebaus. A probabilistic damage detection approach using vibration-based nondestructive testing. *Structural Safety*, 38:11–21, 2012.

[2] Q. Huang, P. Gardoni, and S. Hurlebaus. Adaptive reliability analysis of reinforced concrete bridges subject to seismic loading using nondestructive testing. *ASCE-ASME Journal of Risk and Uncertainty in Engineering Systems, Part A: Civil Engineering*, 1(4):04015014, 2015.

[3] N. M. Okasha, D. M. Frangopol, and A. D. Orcesi. Automated finite element updating using strain data for the lifetime reliability assessment of bridges. *Reliability Engineering & System Safety*, 99:139–150, 2012.

[4] H. Qin and M. G. Stewart. Construction defects and wind fragility assessment for metal roof failure: A Bayesian approach. *Reliability Engineering & System Safety*, 197:106777, 2020.

[5] A. H. de Andrade Melani, M. A. de Carvalho Michalski, R. F. da Silva, and G. F. M. de Souza. A framework to automate fault detection and diagnosis based on moving window principal component analysis and Bayesian network. *Reliability Engineering & System Safety*, 215:107837, 2021.

[6] M. A. Vega, Z. Hu, T. B. Fillmore, M. D. Smith, and M. D. Todd. A novel framework for integration of abstracted inspection data and structural health monitoring for damage prognosis of miter gates. *Reliability Engineering & System Safety*, 211:107561, 2021.

[7] K. V. Yuen. *Bayesian methods for structural dynamics and civil engineering.* John Wiley & Sons, Inc., 2010.

[8] H. Xu and P. Gardoni. Conditional formulation for the calibration of multi-level random fields with incomplete data. *Reliability Engineering & System Safety*, 204:107121, 2020.

[9] Z. Pang, X. Si, C. Hu, D. Du, and H. Pei. A Bayesian inference for remaining useful life estimation by fusing accelerated degradation data and condition monitoring data. *Reliability Engineering & System Safety*, 208:107341, 2021.

[10] J. L. Beck and L. Katafygiotis. Updating models and their uncertainties. I: Bayesian statistical framework. *Journal of Engineering Mechanics*, 124(4):455–461, 1998.

[11] X. Guan, J. He, R. Jha, and Y. Liu. An efficient analytical Bayesian method for reliability and system response updating based on Laplace and inverse first-order reliability computations. *Reliability Engineering & System Safety*, 97(1):1–13, 2012.

[12] C. Papadimitriou, J. L. Beck, and L. S. Katafygiotis. Updating robust reliability using structural test data. *Probabilistic Engineering Mechanics*, 16(2):103–113, 2001.

[13] L. Katafygiotis and J. L. Beck. Updating models and their uncertainties. II: Model Identifiability. *Journal of Engineering Mechanics*, 124(4):463–467, 1998.

[14] C. Robert and G. Casella. *Monte Carlo Statistical Methods.* Springer New York, 2010.

[15] J. Ching, M. Muto, and J. L. Beck. Structural model updating and health monitoring with incomplete modal data using Gibbs sampler. *Computer-Aided Civil and Infrastructure Engineering*, 21(4):242–257, 2006.

[16] N. Metropolis, A. W. Rosenbluth, M. N. Rosenbluth, A. H. Teller, and E. Teller. Equation of state calculations by fast computing machines. *The Journal of Chemical Physics*, 21(6):1087–1092, 1953.

[17] W. K. Hastings. Monte Carlo sampling methods using Markov chains and their applications. *Biometrika*, 57(1):97–109, 1970.

[18] J. L. Beck and S.-K. Au. Bayesian updating of structural models and reliability using Markov chain Monte Carlo simulation. *Journal of Engineering Mechanics*, 128(4):380–391, 2002.

[19] J. Ching and Y.-C. Chen. Transitional Markov chain Monte Carlo method for Bayesian model

updating, model class selection, and model averaging. *Journal of Engineering Mechanics*, 133(7):816–832, 2007.

[20] S. H. Cheung and J. L. Beck. Bayesian model updating using hybrid Monte Carlo simulation with application to structural dynamic models with many uncertain parameters. *Journal of Engineering Mechanics*, 135(4):243–255, 2009.

[21] T. A. Catanach and J. L. Beck. Bayesian system identification using auxiliary stochastic dynamical systems. *International Journal of Non-Linear Mechanics*, 94:72–83, 2017.

[22] M. Betancourt, S. Byrne, S. Livingstone, and M. Girolami. The geometric foundations of Hamiltonian Monte Carlo. *Bernoulli*, 23(4A):2257–2298, 2017.

[23] J.-H. Weng, C.-H. Loh, and J. N. Yang. Experimental study of damage detection by data-driven subspace identification and finite-element model updating. *Journal of Structural Engineering*, 135(12):1533–1544, 2009.

[24] E. Ghorbani and Y.-J. Cha. An iterated cubature unscented Kalman filter for large-DoF systems identification with noisy data. *Journal of Sound and Vibration*, 420:21–34, 2018.

[25] R. Astroza, N. Barrientos, Y. Li, E. I. Saavedra, and Z. Liu. Bayesian updating of complex nonlinear FE models with high-dimensional parameter space using heterogeneous measurements and a batch-recursive approach. *Engineering Structures*, 201:109724, 2019.

[26] D. Straub and I. Papaioannou. Bayesian updating with structural reliability methods. *Journal of Engineering Mechanics*, 141(3):04014134, 2015.

[27] S.-K. Au and J. L. Beck. Estimation of small failure probabilities in high dimensions by subset simulation. *Probabilistic Engineering Mechanics*, 16(4):263–277, 2001.

[28] S.-K. Au and Y. Wang. *Engineering risk assessment with Subset Simulation.* John Wiley & Sons, Inc., 2014.

[29] B. D. Flury. Acceptance–rejection sampling made easy. *SIAM Review*, 32(3):474–476, 1990.

[30] W. Betz, J. L. Beck, I. Papaioannou, and D. Straub. Bayesian inference with reliability methods without knowing the maximum of the likelihood function. *Probabilistic Engineering Mechanics*, 53:14–22, 2018.

[31] F. A. DiazDelaO, A. Garbuno-Inigo, S.-K. Au, and I. Yoshida. Bayesian updating and model class selection with Subset Simulation. *Computer Methods in Applied Mechanics and Engineering*, 317:1102–1121, 2017.

[32] W. Betz, I. Papaioannou, J. L. Beck, and D. Straub. Bayesian inference with Subset Simula-

tion: Strategies and improvements. *Computer Methods in Applied Mechanics and Engineering*, 331:72–93, 2018.

[33] S.-H. Jiang, J. Huang, X.-H. Qi, and C.-B. Zhou. Efficient probabilistic back analysis of spatially varying soil parameters for slope reliability assessment. *Engineering Geology*, 271:105597, 2020.

[34] P. Liu, S. Huang, M. Song, and W. Yang. Bayesian model updating of a twin-tower masonry structure through subset simulation optimization using ambient vibration data. *Journal of Civil Structural Health Monitoring*, 11(1):129–148, 2020.

[35] H.-M. Tian, D.-Q. Li, Z.-J. Cao, D.-S. Xu, and X.-Y. Fu. Reliability-based monitoring sensitivity analysis for reinforced slopes using BUS and subset simulation methods. *Engineering Geology*, 293:106331, 2021.

[36] J. L. Beck and K.-V. Yuen. Model selection using response measurements: Bayesian probabilistic approach. *Journal of Engineering Mechanics*, 130(2):192–203, 2004.

[37] J. A. Hoeting, D. Madigan, A. E. Raftery, and C. T. Volinsky. Bayesian model averaging: A tutorial. *Statistical Science*, 14(4):382–401, 1999.

[38] E. Simoen, C. Papadimitriou, and G. Lombaert. On prediction error correlation in Bayesian model updating. *Journal of Sound and Vibration*, 332(18):4136–4152, 2013.

[39] J. Ching and J.-S. Wang. Application of the transitional Markov chain Monte Carlo algorithm to probabilistic site characterization. *Engineering Geology*, 203:151–167, 2016.

[40] H. A. Jensen, C. Esse, V. Araya, and C. Papadimitriou. Implementation of an adaptive metamodel for Bayesian finite element model updating in time domain. *Reliability Engineering & System Safety*, 160:174–190, 2017.

[41] O. D. Ditlevsen and H. O. Madsen. *Structural reliability methods.* John Wiley & Sons Ltd., Chichester, U.K., 1996.

[42] P.-L. Liu and A. Der Kiureghian. Multivariate distribution models with prescribed marginals and covariances. *Probabilistic Engineering Mechanics*, 1(2):105–112, 1986.

[43] K. M. Zuev, J. L. Beck, S.-K. Au, and L. S. Katafygiotis. Bayesian post-processor and other enhancements of Subset Simulation for estimating failure probabilities in high dimensions. *Computers & Structures*, 92:283–296, 2012.

[44] S.-K. Au and E. Patelli. Rare event simulation in finite-infinite dimensional space. *Reliability Engineering & System Safety*, 148(Supplement C):67–77, 2016.

[45] V. Papadopoulos, D. G. Giovanis, N. D. Lagaros, and M. Papadrakakis. Accelerated subset simulation with neural networks for reliability analysis. *Computer Methods in Applied Mechanics and Engineering*, 223-224:70–80, 2012.

[46] J.-M. Bourinet, F. Deheeger, and M. Lemaire. Assessing small failure probabilities by combined subset simulation and Support Vector Machines. *Structural Safety*, 33(6):343–353, 2011.

[47] Z. Wang and A. Shafieezadeh. Highly efficient Bayesian updating using metamodels: An adaptive Kriging-based approach. *Structural Safety*, 84:101915, 2020.

[48] M. Kitahara, S. Bi, M. Broggi, and M. Beer. Bayesian model updating in time domain with metamodel-based reliability method. *ASCE-ASME Journal of Risk and Uncertainty in Engineering Systems, Part A: Civil Engineering*, 7(3):04021030, 2021.

[49] R. Craig. *Structural dynamics: An introduction to computer methods.* Wiley, New York, 1981.

[50] H. A. Jensen and C. Papadimitriou. *Sub-structure coupling for dynamic analysis: Application to complex simulation-based problems involving uncertainty.* Springer-Verlag GmbH, 2019.

[51] H. A. Jensen, V. A. Araya, A. D. Muñoz, and M. A. Valdebenito. A physical domain-based substructuring as a framework for dynamic modeling and reanalysis of systems. *Computer Methods in Applied Mechanics and Engineering*, 326:656–678, 2017.

[52] P. Angelikopoulos, C. Papadimitriou, and P. Koumoutsakos. X-TMCMC: Adaptive kriging for Bayesian inverse modeling. *Computer Methods in Applied Mechanics and Engineering*, 289:409–428, 2015.

[53] H. A. Jensen, F. Mayorga, and M. A. Valdebenito. On the reliability of structures equipped with a class of friction-based devices under stochastic excitation. *Computer Methods in Applied Mechanics and Engineering*, 364:112965, 2020.

[54] G. Lomiento, N. Bonessio, and G. Benzoni. Friction model for sliding bearings under seismic excitation. *Journal of Earthquake Engineering*, 17(8):1162–1191, 2013.

[55] G. Mosqueda, A. S. Whittaker, and G. L. Fenves. Characterization and modeling of friction pendulum bearings subjected to multiple components of excitation. *Journal of Structural Engineering*, 130(3):433–442, 2004.

[56] C. S. Tsai. Finite element formulations for friction pendulum seismic isolation bearings. *International Journal for Numerical Methods in Engineering*, 40(1):29–49, 1997.

[57] M. Pastor, M. Binda, and T. Harčarik. Modal Assurance Criterion. *Procedia Engineering*, 48:543–548, 2012.